Local Features for Enhancement and Minutiae Extraction in Fingerprints

Hartwig Fronthaler, Klaus Kollreider, and Josef Bigun, *Senior Member, IEEE*

***Abstract*—Accurate fingerprint recognition presupposes robust feature extraction which is often hampered by noisy input data. We suggest common techniques for both enhancement and minutiae extraction, employing symmetry features. For enhancement, a Laplacian-like image pyramid is used to decompose the original fingerprint into sub-bands corresponding to different spatial scales. In a further step, contextual smoothing is performed on these pyramid levels, where the corresponding filtering directions stem from the frequency-adapted structure tensor (linear symmetry features). For minutiae extraction, parabolic symmetry is added to the local fingerprint model which allows to accurately detect the position and direction of a minutia simultaneously. Our experiments support the view that using the suggested parabolic symmetry features, the extraction of which does not require explicit thinning or other morphological operations, constitute a robust alternative to conventional minutiae extraction. All necessary image processing is done in the spatial domain using 1-D filters only, avoiding block artifacts that reduce the biometric information. We present comparisons to other studies on enhancement in matching tasks employing the open source matcher from NIST, FIS2. Furthermore, we compare the proposed minutiae extraction method with the corresponding method from the NIST package, mindtct. A top five commercial matcher from FVC2006 is used in enhancement quantification as well. The matching error is lowered significantly when plugging in the suggested methods. The FVC2004 fingerprint database, notable for its exceptionally low-quality fingerprints, is used for all experiments.**

***Index Terms*—Differential scale space, fidelity, fingerprint restoration, image enhancement, image pyramid, linear symmetry, minutiae extraction, orientation tensor, parabolic symmetry, symmetry features.**

I. Introduction

FOR THE processing of fingerprint images, two stages are of pivotal importance for the success of biometric recognition: image enhancement and feature/minutiae extraction. A topical review of fingerprint processing technologies can be found in [1]. Applied immediately after sensing but before feature extraction, an optional image enhancement can be performed to facilitate the feature extraction and the subsequent processing by "de-noising" the signal. In an ideal fingerprint image, ridges and valleys alternate and flow in a locally constant direction [2]. In realistic scenarios though, the quality of a fingerprint image may suffer from various impairments, caused by 1) scares and cuts, 2) moist or dry skin, 3) sensor noise/blur, 4) wrong handling of the sensor (e.g., too low/high contact pressure), 5) generally weak ridge-valley pattern of the given fingerprint, etc. While not acting against low-quality fingerprints, methods to automatically assess the quality of a given impression, such as [3]–[5], are useful and complementary to this study. The task of fingerprint enhancement is to counteract the aforesaid quality impairments and to reconstruct the actual fingerprint pattern as true to the original as possible. The latter part is especially noteworthy. Furthermore, unrecoverable areas should be labeled as such, since the enhancement at too noisy parts may generate spurious features. There are several published studies on fingerprint image enhancement. Hong *et al.* [6] proposed an algorithm using Gabor bandpass filters tuned to the corresponding ridge frequency and orientation to remove undesired noise while preserving the true ridge-valley structures. All operations are performed in the spatial domain, whereas the contextual filtering in [7] and [8] is done in the Fourier domain. Either way, blockwise processing is used to obtain the enhancement result causing restoration discontinuities at the block boundaries. These methods are likely successful in extremely bad-quality regions, but also rather rigid under easy conditions, due to the radical processing. In [9] and [10], the fingerprint's blockwise Fourier transform is multiplied by its power spectrum raised to a power k, thus magnifying the dominant orientation. A blockwise Fourier transform is also employed by Chikkerur *et al.* [8], [11], followed by contextual filtering using raised cosines. In a related study [12], a standard discrete scale space has been used to contextually process fingerprints. We employ a multigrid representation of a discrete differential scale space following a novel enhancement strategy. For a more detailed review of fingerprint enhancement schemes, we refer to [2].

In this study, we propose the use of an image-scale pyramid and directional filtering in the spatial domain for fingerprint image enhancement to improve the matching performance as well as the computational efficiency. Image pyramids or multiresolution processing is especially known from image compression and medical image processing [13], [14], but their relevance to fingerprint image enhancement has not been quantified before. The Laplacian pyramid [15], [16] is equivalent to bandpass filtering in the spatial domain. Here, we decompose fingerprint images in a similar manner, since we expect all the relevant information to be concentrated within a few frequency bands. Furthermore, we propose Gaussian directional filtering to enhance the ridge-valley pattern of a fingerprint image using

Manuscript received May 8, 2007; revised November 28, 2007. The associate editor coordinating the review of this manuscript and approving it for publication was Dr. Peyman Milanfar.

The authors are with Halmstad University, SE-30118, Halmstad, Sweden (e-mail: hartwig.fronthaler@ide.hh.se; klaus.kollreider@ide.hh.se; josef.bigun@ide.hh.se).

Color versions of one or more of the figures in this paper are available online at http://ieeexplore.ieee.org.

Digital Object Identifier 10.1109/TIP.2007.916155

computationally cheap 1-D filtering on higher pyramid levels (lower resolution) only. The filtering directions are recovered from the orientations of the structure tensor [17], [18] at the corresponding pyramid level. Linear symmetry features are thereby used to extract the local ridge-valley orientation (angle and reliability). In contrast to other studies, e.g., [6] and [11], no blockwise processing is performed, avoiding block boundary artifacts.

Furthermore, we focus on minutia points, which are discontinuities in the ridge flow. The most prominent minutiae are ridge bifurcation and termination (=ending), which refer to points where a ridge divides into two and a ridge ends, respectively. In what follows, we benchmark a recent method to detect the minutiae's position and direction [19]. Existing minutiae extraction approaches comprise so-called "direct grayscale" and "binarization-based" methods. In "binarization-based" methods [20], the fingerprint image is binarized and morphologically analyzed for minutiae. In "direct grayscale" methods, mainly the image gradient and local grayscale neighborhood are used to locate minutiae, either by tracking ridges [21], or by classifying directional filter responses [22]. The direction of a minutia is mostly inherited from the associated ridge. The presented method is a "direct grayscale" approach, as it operates exclusively on the local direction field of a fingerprint image. Note that with partial fingerprints lacking singular points [23] at hand, only local features can be used for alignment and matching purposes. We extend the features used to enhance the image by higher orders sensitive to parabolic symmetry which enable us to detect the minutia points' position and direction. The targeted minutia types are ridge bifurcation and termination. Linear and parabolic symmetry are the only features used throughout our study.

We corroborate our techniques by experiments on a state-of-the-art database for fingerprint recognition, the FVC2004 database [24]. We use the matching module of the NIST FIS2 software [25], [26] to compare our features to the binarization/morphology based features of the software, in an attempt not to favor our features by using a commonly referred matcher. Furthermore, we compare two different fingerprint enhancement methods with our method qualitatively (by human vision) and objectively (via matching performance experiments). We also test the proposed enhancement in conjunction with a top performing matcher of the FVC2006.

II. Local Features

We use two types of symmetries to model and extract the local structure in a fingerprint, which are parabolic and linear symmetry. Both symmetries can be estimated by separable filtering of the orientation tensor. For a more detailed review of symmetry filters, i.e., symmetry derivatives of Gaussians, we refer to [18] and [27]. The starting point for the extraction of our local features is the linear symmetry tensor[1] image, described by the complex expression

$$\begin{aligned} z &= (f_x + if_y)^2 \\ &= [(D_x G(\sigma_1) + iD_y G(\sigma_1)) * f]^2 \end{aligned} \tag{1}$$

[1]It is also known as the structure tensor or the inertia tensor which can be fully represented by (1).

where $i = \sqrt{-1}$, and f_x and f_y denote the derivatives of the image f in x and y direction, respectively. The rightmost part of (1) indicates the actual implementation with a Gaussian bell $G(\sigma_1) = \exp(-(x^2 + y^2)/\sigma_1^2)$, and "$*$" denotes a 2-D convolution. The operations $D_x f$ and $D_y f$ are realized by means of convolutions via $CxG(\sigma_1) * f$ and $CyG(\sigma_1) * f$ (1-D) with C being the nonessential constant $-1/\sigma^2$. The calculation of the tensor implies complex filtering but the synthesis of the complex z happens afterwards at pixel level. This is also true for the symmetry features to be explained next. A symmetry in the image and the associated filter detecting it can be modeled by $\exp(im\phi)$, where m represents its symmetry order [27]–[29]. Parameter m can be any integer, including negative ones. It was shown that to detect a symmetry of type $m \geq 0$ in an image, one can convolve z, described by (1), with the complex filter given by the following polynomial:

$$h_m = (x + iy)^m \cdot \exp\left(-\frac{x^2 + y^2}{2\sigma_2^2}\right). \tag{2}$$

Even symmetries of the type $m < 0$ can be detected in the same way. The corresponding filter is then given by the complex conjugate of the $|m|$-filter in (2). The first type of symmetry used in this study is linear symmetry, which occurs at points of coherent ridge flow. It naturally encodes the local orientation and coherence of the ridge-valley structure as a complex number. The discrimination power of this information has been shown in fingerprint pattern matching [30]. In the case of linear symmetry, which can also be described as symmetry of order $m = 0$ the polynomial in (2) reduces to a Gaussian filter $G(\sigma_2)$, where $\sigma_2 > \sigma_1$. Applying this filter to the orientation tensor $z(x, y)$ corresponds to complex summation/averaging of the linear symmetry tensor in the local neighborhood of each point. To obtain a reliable measure for the linear symmetry, we first calculate the second order complex moments $I_{20} = \langle z, h_0 \rangle$ and $I_{11} = \langle |z|, h_0 \rangle$, as suggested by [17] and [31]. The measure for linear symmetry used in this study is denoted in (3)

$$\mathrm{LS} = \left(\frac{I_{20}}{I_{11}}\right) = \frac{\langle z, h_0 \rangle}{\langle |z|, h_0 \rangle}. \tag{3}$$

Moment I_{11} acts as an upper boundary for the linear symmetry certainty, and by dividing I_{20} through I_{11} unreliable orientations are attenuated, whereas the strong ones are promoted. It is worth noting that linear symmetry detection is also useful for locating minutiae in an inverse fashion, as "lack of linear symmetry" occurs at minutia points [32] (compare Figs. 4 or 6).

Next, we are interested in parabolic symmetry of order $m = 1$, since the parabolic pattern is most similar to a minutia point in a fingerprint. Equation (4) describes how complex filtering is applied to detect this type of symmetry, where $\langle , \rangle$ represents the 2-D scalar product (as before) and $g(x, y)$ denotes the Gaussian window

$$\mathrm{PS} = \langle z, h_1 \rangle = \langle (f_x + if_y)^2, (x + iy) \cdot g(x, y) \rangle. \tag{4}$$

The two grayscale images in Fig. 1 show minutia points of type ridge bifurcation (top) and ridge ending (bottom), with their directions indicated. Next to them, the corresponding complex filter responses of h_1 are displayed. The latter can be described

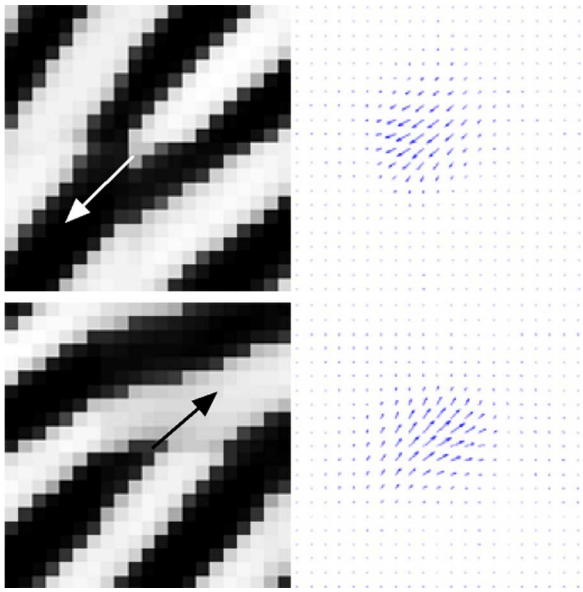

Fig. 1. Parabolic symmetry filter responses PS for (top) ridge bifurcation and (bottom) ridge ending.

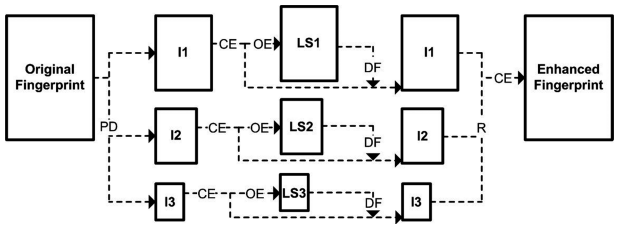

Fig. 2. Data flow: (rectangles) images and (connection labels) applied processing. The abbreviations will become clear within this section.

as $c_1 = \mu \cdot \exp(i\alpha)$. The value μ is a certainty measure and the argument α represents the geometric orientation of the symmetric pattern in symmetry order $m = 1$. An important property of parabolic symmetry filtering for minutiae detection is that the minutia direction is retrieved at the same time (see Fig. 1) as its position, and that this minutia direction estimation is independent of the ridge direction estimation.

Symmetry features of these and higher orders have been useful in a number of tasks in image processing, for example, singular point extraction in fingerprints [33], image quality estimation [3], texture analysis and optical flow estimation [34], recognition of crash test cross trackers [27], etc.

III. Fingerprint Image Enhancement

It has been shown previously that the quality of a fingerprint image directly affects the performance of a given recognition system [3], [24], [35]. In lack of higher quality images, e.g., from a crime scene, or due to worn fingerprints, a carefully undertaken high-fidelity enhancement is frequently the only option that remains to enable identity establishment via fingerprints. The steps involved in the proposed strategy are arranged as illustrated in Fig. 2, each of them to be detailed as follows.

TABLE I
Pyramid Building Process

a) Pyramid Decomposition PD	
Gaussian-like	Laplacian-like
$g_1 = \mathit{reduce}\,(fp, k_0)\,;$	$l_1 = g_1 - \mathit{expand}\,(g_2, k)\,;$
$g_2 = \mathit{reduce}\,(g_1, k)\,;$	$l_2 = g_2 - \mathit{expand}\,(g_3, k)\,;$
$g_3 = \mathit{reduce}\,(g_2, k)\,;$	$l_3 = g_3 - \mathit{expand}\,(g_4, k)\,;$
$g_4 = \mathit{reduce}\,(g_3, k)\,;$	

b) Reconstruction R
$fp = \mathit{expand}\,(..., k_0)\,;$
$\Uparrow \mathit{expand}\,(..., k) + l_1$
$\Uparrow \mathit{expand}\,(l_3, k) + l_2$

A. Pyramid Decomposition (PD)

A pyramid decomposition requires resizing (scaling, or geometric transformation). To create our Gaussian and Laplacian-like pyramids, we define the *reduce* (I, k) and *expand* (I, k) operations, which decrease and increase an image I in size by the factor k, respectively. During *reduce*, the image is initially low-pass filtered to prevent aliasing using a Gaussian kernel.[2] The latter's standard deviation depends on the resizing factor, which here follows the lower bound approximation of the corresponding ideal low-pass filter, $\sigma = (0.75 \cdot k)/(2)$ [18]. We initially *reduce* the original fingerprint image fp by a factor of $k_0 \geq 1.5$ in order to exclude the highest frequencies. In a further step, we *reduce* the image size by a factor $k \leq 1.5$ for three times. This is also outlined on the upper left hand side of Table I. To create images containing only band limited signals of the original image, we *expand* the three images g_{2-4} by factor k and subtract each of them from the next lower level, yielding l_{1-3}. The latter contain the adequately high, medium and low frequencies (ridge-valley pattern) of the original fingerprint. It is worth noting, that only the Laplacian-like pyramid levels l_{1-3} are used subsequently in this study. In a further step, the contrast of the single band images is enhanced, following $l_i = \mathrm{CE}(l_i)$ where $\mathrm{CE}(x) = \mathrm{sign}(x) \cdot \sqrt{|x|}$, to depreciate small vectors of x in comparison with those of large magnitude. Note, that l_i contains no DC content, i.e., ridge pixels have negative values whereas valley pixels are positive (ideally). In Fig. 3, we show example fingerprints of different quality besides their contrast enhanced pyramid levels l_{1-3}. For easier comprehension, the latter are used for an initial reconstruction step, which is displayed rightmost. This reconstruction is crude so far and represents only an isotropic (nondirectional) enhancement, which is implemented as listed at the bottom of **I**. It is already visible that the portions of the fingerprint image that have been retained and contrast improved contain significant recognition information, whereas others containing high-frequency isotropic noise are attenuated.

We cover approximately half the bandwidth of the original image through the bandpass images in total, e.g., by setting k_0 and k to 1.5. This choice depends on the resolution of the fingerprint and normally can be approximated off-line, either experimentally or by using information on the used sensor. In the images studied here the ridge frequency in a fingerprint image

[2]The 2-D Gaussians are the only functions that are Cartesian separable and yet being fully rotational symmetric, avoiding orientation bias [18].

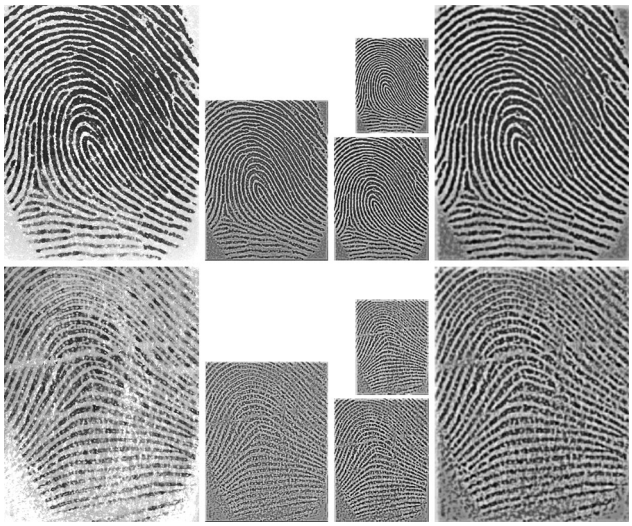

Fig. 3. Pyramid decomposition process of the (top row) high-quality impression 104_6 and a (bottom row) low-quality example 1_1 of the FVC2000-2 dataset; the column images represent 1) the original fingerprint, 2–3) its band-pass like decomposition via l_{1-3} after contrast enhancement, and 4) the "so-far" reconstructed fingerprint.

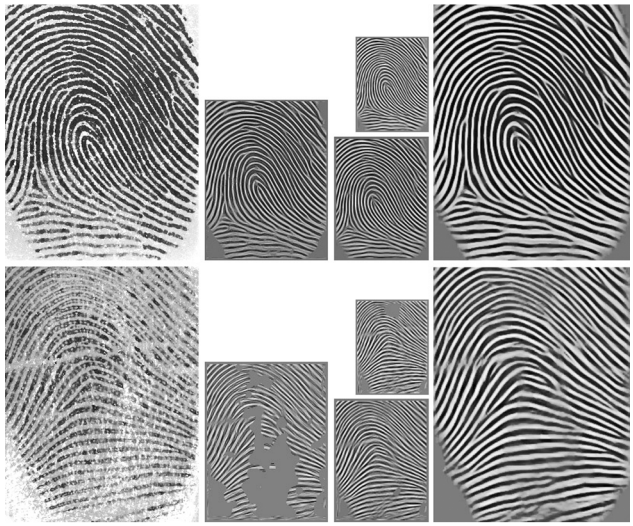

Fig. 5. Directional filtering process of the example fingerprint images featuring high (top row) and a low quality quality (bottom row); the column images represent 1) the original fingerprint, 2–3) directionally filtered pyramid levels l_{1-3} and iv) the final fingerprint after reconstruction and contrast enhancement.

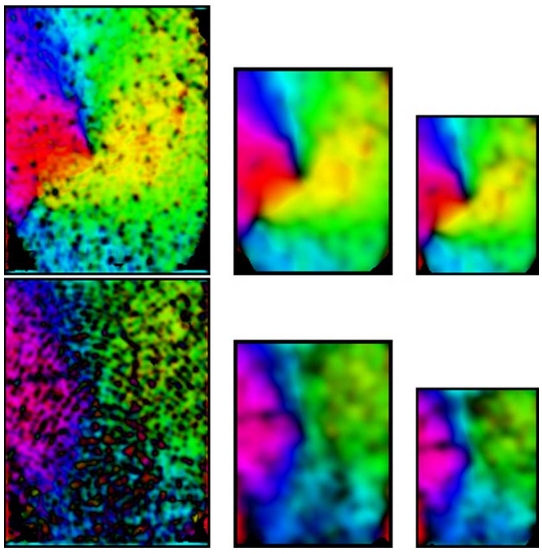

Fig. 4. HSV representation of linear symmetry filter responses LS_{1-3} (columns 1–3) for the two example fingerprints of the FVC2000-2 dataset, where the magnitude steers V and the argument controls H.

is ≈60 cycles per image width/height [6]. This translates to an image dimension of approximately 100–400 pixels for the method to be most effective.

B. Orientation Estimation (OE)

The ridge-valley orientations for each of l_{1-3} are estimated using (3). We calculate $\mathrm{LS}_i = (I_{20})/(I_{11})$ for level i. Being a complex valued image, LS_i encodes the local orientation in a pixel's argument, $\angle \mathrm{LS}_i$, and the reliability of this estimation in the magnitude, $|\mathrm{LS}_i|$. By using LS the measure becomes independent of the signal energy. Furthermore, LS_1 is attenuated if its orientations deviate too much from the ones of LS_2, which is done by $\mathrm{LS}_1 = \mathrm{LS}_1 \cdot |\cos(\angle \mathrm{LS}_1 - \angle \mathrm{LS}_2)|$. This is meaningful because LS_1 contains the most localized orientation (information also at minutia-level), but is also most susceptible to noise. In Fig. 4, LS_{1-3} for the two example fingerprints from 3 are displayed using a HSV model, where the magnitudes modulate value V and the arguments (local orientation) steer hue H. Note the effect of low quality on LS_1, especially in the second row. However, the higher pyramid levels LS_{2-3}, which contain a coarser description of a fingerprint's orientation, are still intact. When compared to a low-pass pyramid (e.g., Gaussian pyramid), the estimated orientations via band-pass pyramids (e.g., Laplacian pyramid) were found noticeably more robust, in this context.

C. Directional Filtering (DF)

To enhance the SNR (signal-to-noise ratio), i.e., to remove sweat pores, scars, etc., we apply directional averaging to all levels l_{1-3} independently, described next. The local filtering direction within l_i is given by $\angle(\mathrm{LS}_i)/2 - \pi/2$, thus it follows the ridges/valleys of the fingerprint. At every point, the neighboring pixels along a line having the same local direction are averaged with a (1-D) Gaussian, yielding the new value. The possible number of different averaging directions is quantized (here 20). Additionally, we exploit the magnitudes of the complex pixels of LS_i. First, pixels where $|\mathrm{LS}_i| < \tau_1$ are assigned to the background, i.e., they are set to 0 (effectively amounting to a segmentation of the fingerprint from the background or the heavily noisy regions). Second, only if $|\mathrm{LS}_i| > \tau_2$ when measured on a small annulus centered at the current pixel, a reasonable quality (presence of ridge-valley pattern at level i) is ensured and the above filtering is done. Otherwise, the pixel is again set to 0. Generally, τ_2 should be chosen higher than τ_1, advisable values are below 0.5. In this pyramidal process, the structure tensors become spatial frequency selective and adaptively steer the smoothing amount and direction along the ridge-valley structures. At the lowest level l_1, fine minutiae are preserved because the LS_1 filtering directions are sensitive to them. At higher

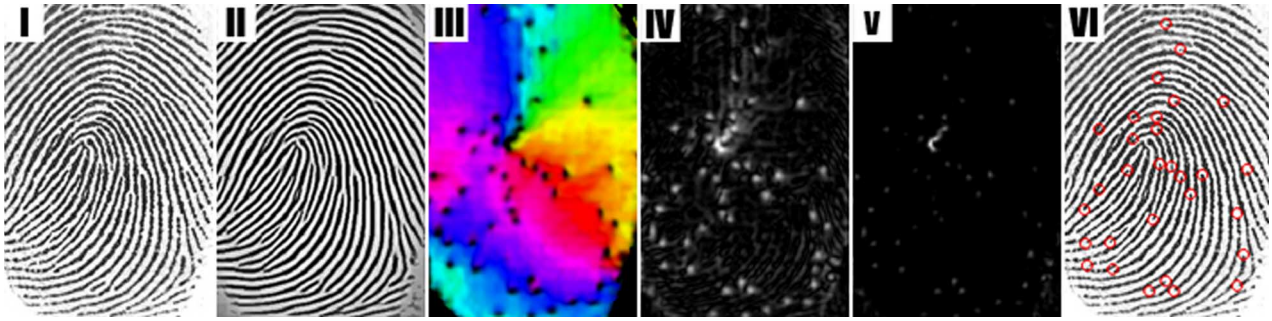

Fig. 6. Minutia point detection process for an example fingerprint; 1) impression 6_0 of the FVC2000-2 dataset and 2) its enhanced version, 3) LS (HSV), 4) $|\mathrm{PS}|$, 5) $|\mathrm{PS}| \cdot (1 - |\mathrm{LS}|)$, 6) 30 strongest minutiae.

levels l_{2-3} the rough ridge-valley flow is smoothed, and gaps are closed (e.g., caused by scars) because LS_{2-3} contain the global orientation. By use of the filtered levels l_{1-3} only, the image is reconstructed (R). A final contrast enhancement (CE) is done subsequently. In Fig. 5, the filtered versions of l_{1-3} for the example fingerprints are displayed besides the reconstructed final, contrast enhanced images. l_1 is most susceptible to noise, which can be observed in the bottom row, where the threshold conditions for τ_1 and τ_2 are not fulfilled in many parts of the potential matching area. Note that in this case, the smoother levels l_{2-3} manage to fill these holes. Singular points like core and delta points do not need further attention during the filtering process, due to the small size of the employed 1-D Gaussians. In Section VI, we will quantify the benefits this fingerprint enhancement affords along with a comparison to alternative strategies.

IV. Fingerprint Minutiae Extraction

Given the enhanced fingerprint image, both LS and PS are computed via (3) and (4) to obtain features to be used in matching. Some more steps have to be considered to reliably detect minutia points. First, the selectivity of the parabolic symmetry filter responses is improved, using the simple inhibition scheme $\mathrm{PS}i = \mathrm{PS} \cdot (1 - |\mathrm{LS}|)$, [36]. Essentially, the parabolic symmetry is attenuated if the linear symmetry is high, whereas it is preserved in the opposite case. In Fig. 6, the minutiae detection process is visualized for an example fingerprint. The first two images depict the initial fingerprint and its enhanced version, respectively. The parabolic symmetry displayed in image IV ($|\mathrm{PS}|$) is inhibited with the absolute value of the linear symmetry shown in image III (LS). The latter image also represents the local orientation. The resulting sharpened magnitudes $|PSi|$ are displayed in image V. In a further, step all filter responses below a certain threshold τ_{PS} are set to zero. LS provides a good measure for segmenting the fingerprint from the background in order to discard responses in the marginal area of the fingerprint image. The remaining filter responses within PSi, which are concentrated to pixel "islands," are used for the extraction of minutia candidates. During this extraction process, we search for the highest filter response in a small neighborhood (here 9×9, determined empirically) throughout the fingerprint area to avoid multiple detection of the same minutia. Finally, we demand each minutia to be fully surrounded by high linear symmetry, by ensuring whether the average linear symmetry on a ring around a minutia candidate is above a threshold τ_{LS}. Thus, we can exclude spurious minutia points which occur at the transition from the fingerprint to the background and at impurities, comprising regions lacking fingerprint structure, e.g., due to low contact pressure, humidity, greasiness, dust, wounds, sensor deficiency, etc., within the fingerprint area. If this condition is fulfilled, the position and the complex filter response are stored. One should set τ_{PS} very close to 0 and τ_{LS} near to 1. The final minutiae list is ordered by magnitude of PS since it represents the presence of parabolic symmetry. In image VI of Fig. 6, the circles indicate detected minutiae when considering only the 30 highest magnitudes.

V. Examples and Qualitative Observations

In this section, we inspect the proposed techniques for enhancement and minutiae extraction visually, including existing methods for both tasks. We discuss the systematic qualitative differences briefly.

First, we show typical examples of enhancement using the proposed method and two other published studies by Hong *et al.* [6] and Chikkerur *et al.* [8], respectively. The implementation of the two latter methods are due to the authors of [8]. Fig. 7 depicts two fingerprint images representing (top row) high- and (bottom row) low-quality from the FVC2004-1 dataset together with their enhanced versions as delivered by the mentioned techniques. The images in the second column, corresponding to the output of [6], are obtained by the use of Gabor-filters, tuned to the estimated spatial frequency and orientation within small blocks of the fingerprint. The filtering is only performed if the corresponding region exhibits sufficient ridge-valley structure according to an estimated signal strength. The results of [8] are visualized in the third column of Fig. 7. Here, all calculations are performed in the frequency domain, using short time fourier transform (STFT), involving small overlapping blocks. The ridge frequency and orientation are determined in the Fourier domain, to steer the contextual filtering by steep bandpass functions. The segmentation of a fingerprint is done by comparing a block's energy to a predetermined threshold. The final column in Fig. 7 depicts the results of the proposed method. As to be expected, our approach does not show block-artifacts because the data processing is not blockwise. Qualitatively, our method produces high contrast between ridges and valleys and the result generally exhibits more fidelity to the original compared to the alternative approaches. The latter can be well observed in the bottom row of Fig. 7, where the alternative approaches

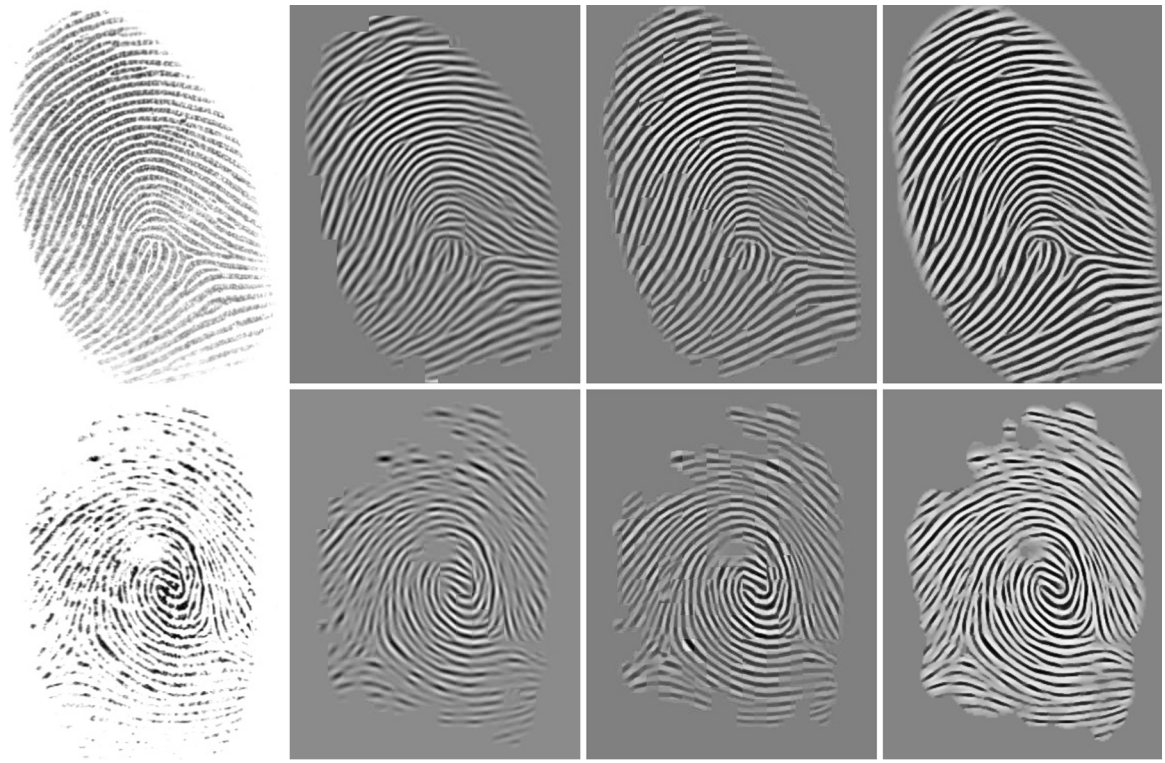

Fig. 7. Enhancement results for the high-quality impression 99_5 (top row) and a low-quality example 1_7 (bottom row) of the FVC2004-1 dataset; the columns correspond to 1) the original image, enhanced by 2) Hong's, 3) Chikkerur's, and 4) the proposed method.

seem to give in (second column) or tamper structure (third column). The images created by the method of [6] (second column) appear more blurred while the ones produced by [8] (third column) contain visible block-artifacts, especially near minutia points. Being the basic resource for most fingerprint recognition techniques, including semiautomatic forensics, it is to be expected that minutia neighborhood degradation will decrease recognition performance.

To provide an initial comparison for the proposed minutiae extraction method, we extract the minutiae with the method suggested by the (US) National Institute of Standards and Technology (NIST, FIS2 mindtct package), [25], [26]. This method takes a fingerprint image, whether pre-enhanced or not, and determines its minutia points fully automatically by means of binarization followed by morphological analysis. The output file contains position, angle, and quality of each detected minutia point. We employ two fingerprint impressions from the FVC2004-3 dataset for a visual comparison, which are shown in the first row of Fig. 8. The first image is of good quality, whereas the second one represents very low-quality conditions intended to pinpoint the limits of both fingerprint image enhancement and minutiae extraction (worst case scenario). The images in the second row of Fig. 8 depict the local minutiae extraction results of the NIST provided method, whereas the third row contains the corresponding result of our minutiae extraction method. Both impressions were pre-enhanced by the introduced method and the detected minutia points are superimposed (rings) on the enhanced fingerprint images. Minutia angles are indicated by directed lines originating from the circles. In the case of (first column) high quality , the method of [25] and [26] detects some spurious, as well as misses some minutiae in comparison to our algorithm. The NIST algorithm quantizes the minutiae angles in $\approx 12^\circ$ intervals, causing visible deviations from the actual minutiae directions. Additionally, the minutiae tend to be imprecisely located with a random error, which is likely due to the information loss during binarization and thinning needed by that method. When facing very low-quality conditions (second column), the enhancement can only recover parts of the original ridge/valley structure with rather low contrast. The NIST provided method is possibly not trained on such images and is, therefore, not able to perform reasonable minutiae extraction in this case. Apart from some spurious and missed minutia points, the proposed method appears to adapt better to these quality conditions. When taking a closer look, five of the detected minutiae are actually valid ones. The others were introduced by enhancement and minutiae detection errors.

Next, we will detail experimental results supporting the qualitative observations above.

VI. Experiments

To quantify the capability of the suggested features and enhancement method we need to test them on very low-quality fingerprint data, where reliable enhancement and minutiae extraction becomes indispensable. Therefore, we use the FVC 2004 database [24], which was collected to provide a more challenging benchmark for state-of-the-art recognition systems than previous fingerprint verification competitions [37]. When collecting the fingerprint data, individuals were asked among other things to vary the contact pressure applied to the sensor

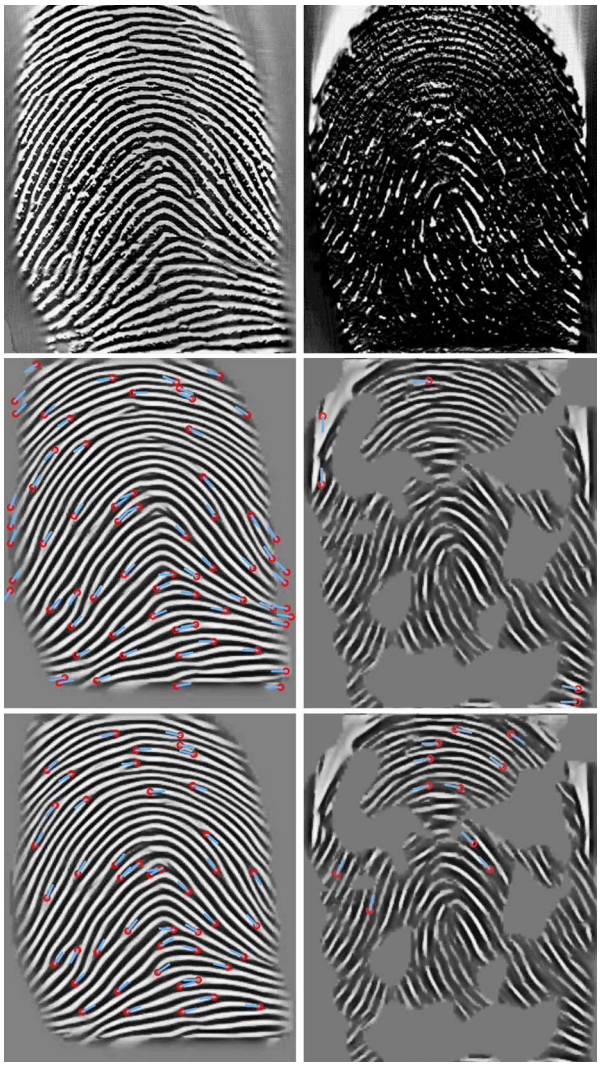

Fig. 8. Minutiae extraction applied to the (left column) high-quality impression 7_1and (right column) a very low-quality example 42_8 of the FVC2004-3 dataset; The three rows show 1) the original fingerprint, minutiae's positions and angles detected by 2) the NIST FIS2 mindtct package versus 3) the proposed method. The fingerprint images were enhanced by our method and the second column shall also indicate its limitations.

and their fingers were additionally dried or moistened to enforce challenging image quality conditions. The FVC 2004 consists of four datasets, which were acquired using different sensor types and each of them contains eight impressions of 100 fingers. Subsequently, we will refer to these datasets as DB1-4. It is worth mentioning that DB4 was created using the SFinGE synthetic fingerprint generator [38] whereas DB1-3 are populated by images representing authentic fingerprints sensed by real sensors. When carrying out fingerprint verification for a single dataset, we follow the FVC protocol involving 2800 genuine trials and 4950 impostor trials.

In our first experiment, we pre-enhanced all fingerprints of DB1-4 with three different enhancement methods: The proposed method, and the ones of Hong [6] and Chikkerur [8], which we already illustrated by way of examples in Section V. We employed the complete NIST FIS2 fingerprint matcher, consisting of a minutiae extractor (the mindtct package) and a method that evaluates the correspondence of the minutiae sets

TABLE II
EERs OF THE NIST FIS2 MATCHER ON THE ORIGINAL AND PRE-ENHANCED FVC2004 DATABASE, FOR DIFFERENT ENHANCEMENT METHODS

Enhancem. Method	DB1	DB2	DB3	DB4
no pre-enhancem.	14,5%	9,5%	6,2%	7,3%
Hong [6]	(16,9%)	14,4%	7,1%	9,8%
Chikkerur [8]	(19,1%)	11,9%	7,6%	10,9%
proposed method	12,0%	8,2%	5,0%	7,0%

TABLE III
EERs, FMR100s, FMR1000s, AND ZEROFMRs OF THE COMMERCIAL MATCHER ON THE ORIGINAL AND PRE-ENHANCED FVC2004 DATABASE

	Original	Pre-enhanced	Change in %	Original	Pre-enhanced	Change in %
	DB1			DB2		
EER	8.1%	6.8%	-16%	3.6%	2.1%	**-41.7%**
FMR100	13%	9.5%	-27%	4.6%	2.5%	**-45.7%**
FMR1000	14.9%	11.6%	-26.2%	5.3%	3%	**-43.4%**
ZeroFMR	16.9%	14.3%	-15.4%	7.4%	4.4%	**-40.5%**
	DB3			DB4		
EER	3.4%	2.9%	-14.7%	2.1%	1.5%	-28.6%
FMR100	5.3%	3.6%	-32.1%	2.5%	1.6%	-36%
FMR1000	7.3%	5.7%	-20.5%	2.9%	1.9%	-34.5%
ZeroFMR	7.9%	7.1%	-10.1%	3.1%	2.1%	-32.3%

of two fingerprints (the bozorth3 package). Needless to say, pre-enhancement should lead to lower error rates for the fingerprint matcher, compared to when trying to match the original fingerprints. Table II shows the equal error rates (EER) of this setup using the full FVC2004 database (all four datasets). The equal error rate marks a system's operating point, at which it erroneously recognizes genuine users and imposters with equal probability. The results in the first row were achieved when using no image enhancement at all. The other rows represent equal error rates in case of all impressions being initially enhanced by the method of Hong (second row), Chikkerur (third row), and by the proposed approach (last row). Interpreting Table II, we conclude that it is not self evident that what is perceived as an enhancement improves the recognition performance. By contrast, there is a significant risk that it actually can worsen (!) the recognition performance, especially when the images are noisy. The method suggested here clearly has led to favorable recognition rates among the tested enhancements, resulting in the lowest EERs on all four datasets. In Section VII, we will discuss the underlying reasons in further detail. No parameters of our enhancement method have been specially adapted to any of the used datasets, neither were the others. Studying the matching failures, we could conclude that the fingerprint area useful for recognition sometimes happened to be very small, when enhanced by the other methods (especially in DB1). This is indicated by the parentheses in Table II.

As to signal enhancement, it may seem easy to improve recognition rates of a modest matcher, or to show qualitative advantages over other research prototypes. For these reasons, we assisted fingerprint recognition systems which were already state-of-the-art in all respects. A top five matcher of the FVC 2006 benchmark, termed commercial matcher below, was reevaluated on fingerprints that were pre-enhanced by our method. Following the FVC evaluation style, we show full ROC curves and explicitly list some operating points in this case. Three such points are particulary important, besides the EER, the FMR 100, FMR 1000, and ZeroFMR. FMR stands for false

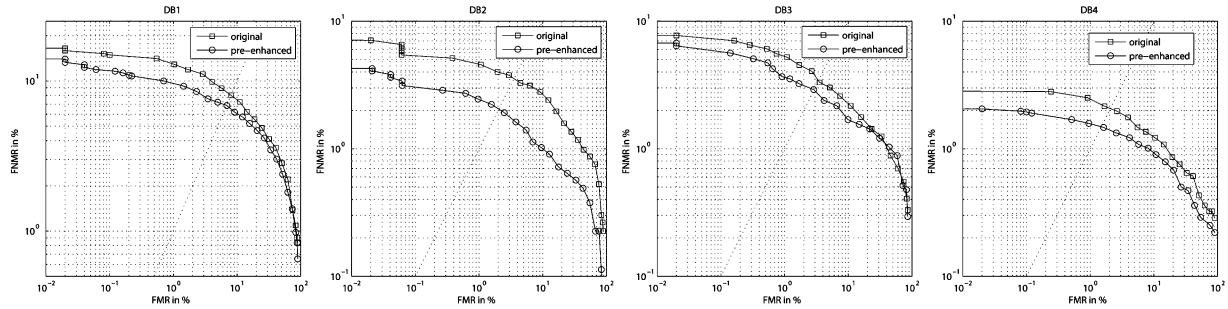

Fig. 9. ROC curves of the commercial matcher on the original and pre-enhanced (by the proposed method) datasets of FVC2004. The EER is to be read off at the intersection point between a curve and the diagonal line.

match rate, the probability of an impostor being erroneously recognized as genuine user. Furthermore, FMR 100, FMR 1000 and ZeroFMR are popular marks meaning 1 false match in 100 trials, 1 in 1000 and 0 such erroneous decisions. The lowest false nonmatch rate (FNMR) that a system can achieve when its FMR is below or equal to the mentioned amounts, is represented by these three indicators. In other words, they determine how often a genuine user is not recognized as such, at a certain security level, and are sometimes given more significance than the EER by systems used in practice. This is because these measures are more indicative for the user annoyance to be expected. In Table III, we have listed the recognition rates of the commercial matcher on the original and pre-enhanced datasets DB1-4. Next to these, we show the relative variation between each pair of rates (columns *Original* serve as reference). The enhancement method was the one proposed, with the difference that the downsize factors $f_0 - f_3$ had been adjusted once to match the fingerprints (dimensions) more accurately. Recalling Table II, one can observe that the commercial matcher achieves remarkably lower EERs than the one of NIST. This behavior is valid also at other operating points. We omitted an explicit list of those since the purpose here is not to compare the two matchers, though. Studying Table III reveals that the proposed enhancement leads to decreased error rates of the commercial matcher at all listed operating points and on each of the tested datasets. The best results were observed on dataset DB2 (highlighted column), for which the error rates dropped by over 40%, measured in percentage point drop-off. In Fig. 9, we further show the corresponding receiver operator characteristics (ROC) curves, which extend the analysis to all possible operating points. The axes of such a plot represent the false match and false non match rates. Note, that the EER of a system can be read off at the point where its curve intersects with the diagonal line. As can be observed in Fig. 9, the commercial matcher benefits from the pre-enhanced images in that the drop-off in error rates is significant and occurs at all relevant operating points across all the four datasets.

In our third experiment, we have studied the performance of the proposed minutiae extraction. To be precise, we have compared the minutiae extracted by the proposed method with those of NIST FIS2 (mindtct), quantitatively. We used the fingerprints enhanced by the introduced method from our first experiment above, as they led to the best recognition results using the independent NIST matcher. Feeding the minutiae, as extracted by our method, to the NIST minutiae matcher (bozorth3) is not less than fair because one would assume that the latter was designed to cope best with its own minutiae. It is also worth noting that there are many ways of doing a matching given two sets of minutiae [39], and that this was the only way available to us of quantifying the proposed technique for minutiae extraction. In Table IV, second row, the corresponding EERs, employing the proposed minutiae extraction method are given, whereas we restate the error rates involving the NIST feature extraction in the first row (the top row of Table IV and the bottom row of Table II are naturally the same). We can observe that the proposed scheme for minutiae extraction leads to improved recognition on all four datasets. The improvements are substantial and meaningful because neither of the methods (for enhancement and minutiae extraction) were specially adapted to any of the tested datasets or the NIST matching module.

TABLE IV
EERs OF THE NIST MATCHER WHEN USING ITS OWN MINUTIAE VERSUS USING MINUTIAE EXTRACTED BY THE SUGGESTED METHOD. THE FVC2004 DATABASE IMAGES WERE PRE-ENHANCED BY THE METHOD PRESENTED IN SECTION III IN BOTH CASES

Minutiae Extraction Method	DB1	DB2	DB3	DB4
NIST FIS2 mindtct	*12,0%*	*8,2%*	*5,0%*	*7,0%*
Proposed method	9.8%	7,3%	4,4%	6,1%

VII. DISCUSSION

Generally, it is difficult to quantify the advantages of local features used for recognition, other than by the success of known procedures and contexts employing them. Using such procedures on publicly available databases allows testing the methods in numerous contexts of the reality, in addition to that the tests can be repeated by others, and/or there can be a comparison at the output level, e.g., recognition performance, without an implementation. If one had the ground truth (de-noised images or minutiae positions and angles) for a database, additional testing strategies would have been possible. Unfortunately, there are no such datasets available because annotated databases are difficult to acquire.

Beside the datasets used, we had a set of rolled fingerprints out of NIST's special database 14 at our disposal. After a rough adaptation to the ridge frequency of the fingerprints, the proposed methods led to higher recognition rates than NFIS2 in initial experiments. The fingerprint pattern area is naturally larger in case of rolled fingerprints and, thus, contains a lot

more minutia points, which increases the recognition potential substantially. Also in terms of impression quality, the FVC 2004 is regarded as more challenging than all earlier collected fingerprint databases. Since we wanted to show the benefits of our algorithms on more difficult fingerprint data, we did not give an account of performance with rolled fingerprints.

Our experiments showed that even a commercial grade matcher can benefit from pre-enhancement. We conclude that this is only possible if the latter truly preserves signal fidelity—in other words, if the enhancement does not distort the fingerprint's minutiae or texture. The reason for why the other enhancement methods did not perform equally well is not that they cannot deliver a meaningful enhancement as it is beyond doubt that their ability has been well demonstrated in published studies. However, it is to the best of our knowledge the first time that they have been tested on a highly corrupted database which poses greater challenges on the underlying assumptions and side effects of the image processing.

A benefit of the proposed techniques is that they are possible to implement via fast signal processing techniques (1-D filtering, pyramidal processing, etc.,) applied directly to the original grayscale images, avoiding morphological operations all together. The latter also adds not the least to the accurateness of the minutia extraction. Finally, our local features could also provide added value (complementary information) in nonminutiae based fingerprint recognition systems. The parabolic symmetries reinforce the minutia definition and the linear symmetries describe the texture outside of the minutia area, useful for orientation matching in texture based fingerprint analysis.

VIII. Conclusion

Symmetry features for local fingerprint image processing have been presented and exploited in a novel image enhancement procedure as well as for reliable minutiae extraction. The enhancement is applied progressively, i.e., blockwise operations are avoided, in the spatial domain. It does naturally not suffer from blocking artifacts. Both absolute frequency (granularity or isotropic frequency) and orientation (nonisotropic information) of the fingerprint pattern are utilized to obtain the enhancement. The former is implemented by exploiting several levels of a bandpass pyramid and treating them independently. The typical ridge-valley flow is coherence enhanced by using directional averaging and the structure tensor direction (linear symmetry features) at each level. The processing of the lowest level adds to the fidelity and details (conservation of minutiae) whereas the rough ridge-valley flow is cleaned and gaps are closed at higher levels. Furthermore, the suggested minutiae extraction handles both ridge bifurcation and endings and employs features from the enhancement, with addition of parabolic symmetry features. They allow for simultaneous detection of the minutiae's position and direction. One-dimensional filtering is applicable for all tasks. The suggested local features can provide ridge-valley texture information also to nonminutiae based systems. Comprehensive test results on challenging datasets (FVC2004) are favorable to the suggested methods: A standardized minutiae matcher from NIST achieves the lowest equal error rate if the fingerprints are pre-enhanced by our strategy. If we additionally replace its minutiae extraction with the proposed one, the error rates are decreased even further. Similarly, we have evaluated a commercial matcher in conjunction with the suggested enhancement method. The results support that even state-of-the-art fingerprint recognition systems benefit from the proposed techniques.

Acknowledgment

The authors would like to thank the reviewers for their suggestions on experimental evaluation.

References

[1] A. K. Jain, S. Pankanti, S. Brabhakar, and A. Ross, "Recent advances in fingerprint verification," in *Audio and Video-Based Biometric Person Authentication*, J. Bigun and F. Smeraldi, Eds. New York: Springer, 2001, pp. 182–191.

[2] D. Maltoni, D. Maio, A. K. Jain, and S. Prabhakar, *Handbook of Fingerprint Recognition*. New York: Springer, 2003, includes DVD-ROM.

[3] H. Fronthaler, K. Kollreider, and J. Bigun, "Automatic image quality assessment with application in biometrics," in *Proc. IEEE Workshop on Biometrics*, New York, Jun. 2006, pp. 30–35.

[4] E. Tabassi, C. Wilson, and C. Watson, "Fingerprint image quality," Tech. Rep. NISTIR7151, 2004.

[5] Y. Chen, S. Dass, and A. Jain, "Fingerprint quality indices for predicting authentication performance," in *Proc. Audio- and Video-based Biometric Person Authentication*, Jul. 2005, pp. 160–170.

[6] L. Hong, Y. Wand, and A. Jain, "Fingerprint image enhancement: Algorithm and performance evaluation," *IEEE Pattern Anal. Mach. Intell.*, vol. 20, no. 8, pp. 777–789, Aug. 1998.

[7] B. G. Sherlock, D. M. Monro, and K. Millard, "Fingerprint enhancement by directional fourier filtering," *Vis. Image Signal Process.*, vol. 141, no. 2, pp. 87–94, 1994.

[8] S. Chikkerur and V. Govindaraju, "Fingerprint image enhancement using STFT analysis," in *Proc. Int. Workshop on Pattern Recognition for Crime Prevention, Security and Surveillance*, 2005, pp. 20–29.

[9] C. I. Watson, G. T. Candela, and P. J. Grother, "Comparison of FFT fingerprint filtering methods for neural network classification," *NISTIR*, vol. 5493, 1994.

[10] A. Willis and L. Myers, "A cost-effective fingerprint recognition system for use with low-quality prints and damaged fingerprint," *Pattern Recognit.*, vol. 34, no. 2, pp. 255–270, Feb. 2001.

[11] S. Chikkerur, C. Wu, and V. Govindaraju, "A systematic approach for feature extraction in fingerprint images," in *Proc. Int. Conf. Bioinformatics and its Applications*, 2004, pp. 344–350.

[12] A. Almansa and T. Lindeberg, "Fingerprint enhancement by shape adaptation of scale-space operators with automatic scale-selection," *IEEE Trans. Image Process.*, vol. 9, no. 12, pp. 2027–2042, Dec. 2000.

[13] H. F. D. Kunz, K. Eck, and T. Aach, "A nonlinear multi-resolution gradient-adaptive filter for medical images," in *Proc. SPIE Medical Imaging*, 2003, vol. 5032, pp. 732–742.

[14] D. Kaji, "Improvement of diagnostic image quality using a frequency processing based on decomposition into multiresolution space -hybrid processing," MI Solution Group, Tech. Rep., 2002.

[15] E. H. Adelson, C. H. Anderson, J. R. Bergen, P. J. Burt, and J. M. Ogden, "Pyramid methods in image processing," *RCA Eng.*, vol. 29, no. 6, pp. 33–41, 1984.

[16] E. P. Simoncelli and W. T. Freeman, "The steerable pyramid: A flexible architecture for multi-scale derivative computation," in *Proc. Int. Conf. Image Processing*, Washington, DC, Oct. 1995, vol. 3, pp. 23–26.

[17] J. Bigun and G. H. Granlund, "Optimal orientation detection of linear symmetry," in *Proc. 1st Int. Conf. Computer VisionLondon*, Washington, DC, 1987, pp. 433–438.

[18] J. Bigun, *Vision With Direction*. New York: Springer, 2006.

[19] H. Fronthaler, K. Kollreider, and J. Bigun, "Local feature extraction in fingerprints by complex filtering," in *Proc. Int. Workshop on Biometric Recognition Systems*, Beijing, China, Oct. 22–23, 2005, vol. 3781, pp. 77–84.

[20] A. Jain, L. Hong, and R. Bolle, "On-line fingerprint verification," *IEEE Pattern Anal. Mach. Intell.*, vol. 19, no. 4, pp. 302–314, Apr. 1997.

[21] D. Maio and D. Maltoni, "Direct gray-scale minutiae detection in fingerprints," *IEEE Pattern Anal. Mach. Intell.*, vol. 19, no. 1, pp. 27–40, Jan. 1997.

[22] M.-T. Leung, W. Engeler, and P. Frank, "Fingerprint image processing using neural networks," in *Comput. Commun. Syst.*, Sep. 24–27, 1990, pp. 582–586.
[23] K. Nilsson and J. Bigun, "Localization of corresponding points in fingerprints by complex filtering," *Pattern Recognit. Lett.*, vol. 24, pp. 2135–2144, 2003.
[24] D. Maio, D. Maltoni, R. Cappelli, J. Wayman, and A. Jain, "FVC 2004: Third fingerprint verification competition," in *Proc. Int. Conf. Biometric Authentication*, Hong Kong, Jul. 2004, pp. 1–7.
[25] *Home Page of NIST*, [Online]. Available: http://www.itl.nist.gov/div894/894.01/online.htm
[26] C. I. Watson, M. D. Garris, E. Tabassi, C. L. Wilson, R. M. McCabe, and S. Janet, "User's guide to fingerprint image software 2–NFIS 2," *NIST*, 2004.
[27] J. Bigun, T. Bigun, and K. Nilsson, "Recognition by symmetry derivatives and the generalized structure tensor," *IEEE Pattern Anal. Mach. Intell.*, vol. 26, no. 12, pp. 1590–1605, Dec. 2004.
[28] J. Bigun, "Recognition of local symmetries in gray value imagesby harmonic functions," in *Proc. 9th Int. Conf. Pattern Recognition*, Rome, Italy, Nov. 14–17, 1988, pp. 345–347.
[29] H. Knutsson, M. Hedlund, and G. H. Granlund, "Apparatus for determining the degree of consistency of a feature in a region of an image that is divided into discrete picture elements," U.S. patent, 4.747.152, 1988.
[30] J. Bigun, H. Fronthaler, and K. Kollreider, "Assuring liveness in biometric identity authentication by real-time face tracking," in *Proc. IEEE Int. Conf. Computational Intelligence for Homeland Security and Personal Safety*, Venice, Italy, Jul. 21–22, 2004, pp. 104–112.
[31] M. Kass and A. Witkin, "Analyzing oriented patterns," *Comput. Vis, Graph., Image Process.*, vol. 37, pp. 362–385, 1987.
[32] K. Nilsson and J. Bigun, "Using Linear Symmetry Features as a Pre-Procesing Step for Fingerprint Images," in *Audio and Video Based Person Authentication-VBPA 2001*, J. Bigun and F. Smeraldi, Eds. New York: Springer, 2001, pp. 247–252.
[33] K. Nilsson, "Symmetry filters applied to fingerprints," Ph.D. dissertation, Chalmers Univ. Technol., Göteborg, Sweden, 2005.
[34] J. Bigun, G. H. Granlund, and J. Wiklund, "Multidimensional orientation estimation with applications to texture analysis and optical flow," *IEEE Pattern Anal. Mach. Intell.*, vol. 13, no. 8, pp. 775–790, Aug. 1991.
[35] J. Fierrez-Aguilar, L.-M. Munoz-Serrano, F. Alonso-Fernandez, and J. Ortega-Garcia, "On the effects of image quality degradation on minutiae- and ridge-based automatic fingerprint recognition," presented at the IEEE Int. Conf. Security Technology, Oct. 2005.
[36] B. Johansson, "Multiscale curvature detection in computer vision," M.S. thesis, Linköping Univ., Linköping, Sweden, 2001.
[37] R. Cappelli, D. Maio, D. Maltoni, J. L. Wayman, and A. K. Jain, "Performance evaluation of fingerprint verification systems," *IEEE Pattern Anal. Mach. Intell.*, vol. 28, no. 1, pp. 3–18, Jan. 2006.
[38] R. Cappelli, D. Maio, and D. Maltoni, "Synthetic fingerprint-image generation," presented at the Int. Conf. Pattern Recognition, 2000.
[39] N. K. Ratha and R. Bolle, *Automatic Fingerprint Recognition Systems*. New York: SpringerVerlag, 2003.

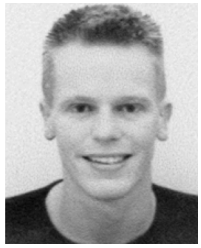

Hartwig Fronthaler received the M.S. degree from the Department of Computer Systems Engineerin, Halmstad University, Sweden.

His specialization has been in the field of image analysis with a focus on biometrics. He joined the signal analysis group of Halmstad University in 2004. His major research interests are in the field of fingerprint processing, including automatic quality assessment and feature extraction. Furthermore, he has been involved in research on face biometrics.

Klaus Kollreider received the M.S. degree in computer systems engineering from Halmstad University, Sweden, in 2004, after which he joined its signal analysis group.

His scientific interests include signal analysis and computer vision, in particular, face biometrics and anti-spoofing measures by object detection and tracking. He is involved in a European project focused on biometrics, BioSecure, where he has also contributed to a reference system for fingerprint matching.

Josef Bigun (M'88–SM'98) recieved the M.S. and Ph.D. degrees from Linköping University, Sweden, in 1983 and 1988, respectively.

Between 1988 and 1998, he was with the EPFL, Switzerland. He was elected Professor to the Signal Analysis Chair at Halmstad University and the Chalmers University of Technology in 1998. His scientific interests include a broad field in computer vision, texture and motion analysis, biometrics, and the understanding of biological recognition mechanisms.

Dr. Bigun has cochaired several international conferences. He has been contributing as a referee or as an editorial board member of journals including *Pattern Recognition Letters* and the IEEE TRANSACTIONS ON IMAGE PROCESSING. He served on the executive committees of several associations, including IAPR. He has been elected Fellow of IAPR.